Aggravation of Airway Inflammation in RSV-Infected Asthmatic Mice Following Infection-Induced Alteration of Gut Microbiota

Jing wang[1], Huina Lu[2], Linlin yu[1], Weiwei Cheng[1], Wuning yan[1], and xiaoping jing[1]

[1]Shanghai Jiaotong University Children's Hospital
[2]Chongqing City Hospital of Traditional Chinese Medicine

October 12, 2020

Abstract

This investigation was to confirm the relationship between asthma, respiratory syncytial virus (RSV) infection, and the gut environment by analyzing the alterations in the gut microbiota of RSV-infected asthmatic mice. All BALB/c male mice were randomly separated into the control group (CON), ovalbumin (OVA) group, and OVA + RSV group (n = 8). At the end of experiment, we evaluated the RSV-infected asthma model using Wright-Giemsa staining, immunoglobulin E (IgE) levels using ELISA, and inflammatory cells using Hematoxylin and eosin (HE). Furthermore, airway hyperresponsiveness (AHR) was measured by a Buxco's modular and invasive system. Histopathological analysis of the murine lung tissue revealed that the inflammatory infiltration, edema, and collagen hyperplasia were more severe in the OVA + RSV group than in the other groups. Higher expression of interleukin-5 (IL-5), IL-13, IL-25, and IL-33 in mice from the OVA and OVA + RSV groups (*P < 0.05 and **P < 0.01). Moreover, feces were collected for 16S rRNA sequencing and data analysis. The associations between Prevotellaceae_UCG_001, which is positive, and immunoglobulin E (IgE), IL-13, and IL-33 were highly significant (***P < 0.001), IL-5 (**P < 0.01) and IL-25 (*P < 0.05). Lachnospiraceae_NK4A136_group was also positive, and significantly associated with IgE and IL-33. Helicobacter and Uncultured_Bacteroidales_bacterium are negative, had associated with IL-25 (*P < 0.05). Thus, we conclude that asthma with RSV infection can alter the major components of gut microbiota and influence the mutual relationship between the core operational taxonomic units (OTUs) and IgE as well as inflammatory cytokines.

Introduction

Asthma is a chronic disease affecting children with variable expiratory airflow limitation; some of its symptoms include wheezing, shortness of breath, chest tightness, and cough due to chronic airway inflammation[1]. According to Global Institute for Asthma (GINA) Committee and the International Study of Asthma and Allergies in Childhood (ISAAC) Phase Three Study Group, 300 million people are affected with asthma and 4.9% of children have symptoms of severe asthma worldwide, with 3.2% cases in Asia-Pacific region[1-2]. The incidence, prevalence, and disability-adjusted life years (DALYs) of childhood asthma still continue to grow in China [3-4].

Respiratory syncytial virus (RSV) is a negative-sense single stranded RNA virus of the *Paramyxoviridae* family [5], and is the most common respiratory pathogen. RSV infection can promote airway obstruction and recurrent wheezing leading to damage of the airways, which is a huge disease burden in infants and young children worldwide [6]. On the other hand, asthma can also lead to more frequent and severe RSV infection [7]. Asthma with RSV infection can release multiple mediators and cytokines that amplify the inflammatory response in the structural cells of the asthmatic airways and participate in the structural changes in airways. This leads to induction of mucus hypersecretion, subepithelial fibrosis, and an increase in smooth muscles and blood vessels in the airway walls. Taken together, these changes result in airway narrowing and airway hyperresponsiveness (AHR) [7-9].

Gut microbiota comprises bacteria colonizing the gastrointestinal tract and represent 10^{14} bacterial species in the human gut[10]. Healthy gut flora can promote nutrient metabolism and the growth of the mucosa, which is mainly related to the overall health of the host [11]. Recent studies found that a change in the quantity, type, and maturation of gut microbiota at 3 months of age is a very important factor affecting the development of asthma and atopy in childhood [12-13]. Notably, symptoms of digestive system diseases, such as vomiting, diarrhea, and abdominal pain have been observed in patients with corona virus disease 2019 (COVID-19), the ongoing pandemic with a mortality rate of 1.4%[14]. These findings conform with the theory of 'gut-lung axis,' which is a research has linked changes in the gut microbiome with lung inflammation, as lung infection can disrupt the gut microbiota via the blood circulator system [15]. However, whether infection of asthmatic patients with RSV impacts their gut microbiota and the mechanisms underlying this phenomenon remain unclear. In this study, we created an RSV infected asthma model and studied the relationship among immunoglobulin E (IgE), airway inflammation, and gut microbiota using histopathology, ELISA, and 16S rRNA sequencing.

MATERIALS AND METHODS

Preparation of RSV

RSV was prepared according to the method described by Yan Sun[16] with slight modifications. RSV A2 strain (ACTT, USA) was inoculated in Hep-2 cells overspreading 80%-90% of the visual field, which were cultured in DMEM (Gibco, Australia, 2036226) at 37 °C with 5% CO_2. The RSV laden cells were washed twice. The cell culture flask was gently shaken for 15-30 min, 4 times, to remove the unbound RSV and the cells were further fostered in the incomplete medium with 2% fetal bovine serum and 1% penicillin-streptomycin in the same environment. When incidences of syncytia formation, cell death, or floating cells were observed after 3-5 days, the supernatant was harvested in centrifuge tubes. Subsequently, three cycles of freeze-thaw at -80 degC and 37 degC were rapidly carried out, followed by vortexing after every cycle. Then, the supernatants were centrifuged at 300 xg for 10 min at 4 degC, and the filtrate was filtered using a 0.45 μm filter, then rapidly frozen in liquid nitrogen and stored at –80 °C.

RSV infected asthma model

Six-to-eight weeks old BALB/c male mice (Shanghai SLAC Laboratory Animal Co., Ltd) were given standard diet and maintained at light/dark cycle and 24 ± 2 °C, 46 ± 5% humidity. After 5 days of acclimatization, 24 mice were randomly divided into the control groups (CON) (n = 8), ovalbumin (OVA) (n = 8), and OVA + RSV groups (n = 8). The asthma model was sensitized via intraperitoneal injections (i.p.) of OVA (grade V, Sigma) (OVA 20 μg + $AL(OH)_3$ 2 mg, 0.2 mL) at 0, 14, and 28 days. Then, the mice inhaled 1% OVA (grade V, Sigma) + PBS via a 402 AI ultrasonic atomizer (Shanghai Yuyue Medical Equipment Co., Ltd.) from day 22 to day 30 for 15 min (15 mL twice, to prevent suffocation). The OVA and OVA + RSV groups received consecutive infections of RSV (1.0×10^6 PFU·mL^{-1}, 50 μL) in the morning of days 28, 30, and 32, while the mice from the normal control group were administered PBS (**Figure. 2 A**). After 24 h of the last administration, bronchoalveolar lavage (BAL) fluid were collected for Wright-Giemsa stain, airway hyperresponsiveness was tested, and murine lung tissues were collected for examining inflammatory changes using HE, PAS, and VG staining. Serum levels of interleukins were analyzed using ELISA. Samples from large intestine and feces were collected for 16S rRNA sequencing.

Bronchoalveolar lavage fluid (BALF)

After lung function assessment, mice were sacrificed by administering sodium pentobarbitone (2.5%) and cannulating the trachea. Then, BAL obtained from the airway lamina was washed with 1.0 ml sterile PBS. Cell types were determined and 100 mL fluid was deposited onto glass slides using cytospin for Wright-Giemsa stain. Differential cell counts were determined from 200-600 leukocytes using standard hematological criteria. The BALF supernatant was stored at -25 .

Airway hyperresponsiveness (AHR)

AHR was measured with a Buxco's modular and invasive system (Buxco Electronics Inc., NY, USA). Pul-

monary airway resistance (RL) and lung dynamic compliance (Cdyn) were tested directly as described previously[17]. The anesthetized mice were tracheostomized and intubated with a special cannula, then laid in the supine position inside a plethysmograph chamber. After a stable baseline airway pressure was achieved, the mice were successively administered aerosolized PBS. Then, the values were recorded in response to increasing concentrations of methacholine (3.125, 6.25, and 12.5 mg/mL) and expressed as a percentage change from the baseline value.

Histology

Lung tissues from the mouse model were fixed in 4% buffered paraformaldehyde overnight, embedded in paraffin, and sliced (Leica, Germany, RM2235) into 4 μm sections. HE, PAS, and VG staining were used to observe discrepancies in the lung tissue. The slices were then viewed under a light microscope using high magnification (100×) (Leica, Germany, BX42).

ELISA

Blood of mice was collected after 2 h at 20-25 , then centrifuged for 30 min at 1200 x g / 4 to isolate the serum. The levels of the inflammatory factors IgE, IL-5, IL-13, IL-25, and IL-33 were analyzed using ELISA according to the manufacturer's instructions (USCN Business Co., Ltd., China).

16S rRNA Sequencing

Isolated genomic DNA from fecal samples of RSV-infected mice were PCR amplified for the V3-V4 hypervariable regions of the bacterial 16S rRNA. The reaction was carried out in a 25 μL volume using universal primer pairs (343F: 5'-TACGGRAGGCAGCAG-3'; 798R: 5'-AGGGTATCTAATCCT-3'). Both primers were connected with an illumina sequencing adapter. The reaction conditions were as follow: 94 °C for 5 min; 26 cycles at 94 °C for 30 s, 56 °C for 30 s, 72 °C for 5 min.

The amplicons were purified with AMPure XP beads, visualized using gel electrophoresis, and amplified for a second round of PCR. After the amplicon purification by using the AMPure XP beads, the final amplicon was quantified by Qubit dsDNA assay kit. Equal quantities of purified amplicon were pooled for sequencing. Two paired-end read cycles of 300 bases each to sequence were performed on an Illumina Miseq (Illumina Inc., USA).

Bioinformatics

To detect and cut off ambiguous bases (N), paired-end reads were preprocessed using Trimmomatic software [18]. Reads with low quality score (below 20) were cut off using trimming the approach. Then, paired-end reads were assembled by FLASH software[19]. The assembly parameters were: 10 bp of minimal overlapping, 200 bp of maximum overlapping, and 20% of maximum mismatch rate. Further denoising of the sequencing data was performed as follows: reads with ambiguous, homologous sequences, or below 200 bp were not considered. Seventy-five percent of bases above Q20 were retained using QIIME1.8.0 software [20]. Then, the reads with chimera were detected and removed using UCHIME [21]. Clean reads were subjected to primer sequence removal and clustering to generate operational taxonomic units (OTUs) using VSEARCH software with a 97% similarity cut off [22]. Each OTU was selected using the QIIME package. All representative reads were annotated and blasted against the Silva database (Version 123) using a RDP classifier (confidence threshold was 70%) [23]. The microbial diversity of fecal samples in RSV-infected mice was estimated using the alpha diversity that include the Chao1 [24] and Shannon indexes [25]. The Bray Curtis distance matrix was generated using QIIME software, which also provides the Bray Curtis Principal coordinates analysis (PCoA) and phylogenetic tree construction. The 16S rRNA sequencing and analysis were conducted by OE Biotech Co., Ltd, Shanghai, China.

Data availability

All bacterial sequencing data of 16S rRNA gene generated in this study were deposited in the NCBI (National Center for Biotechnology Information) Sequence Read Archive under the accession number PRJNA627257, (http://www.ncbi.nlm.nih.gov/sra).

Statistical analysis

All data were statistically analyzed and presented as mean ± standard deviation (SD) using GraphPad Prism V5. The three groups were analyzed using repeated one-way analysis of variance (ANOVA) and multiple comparison post-hoc tests. The ELISA comparisons between two groups were analyzed using variance analysis. $P < 0.05$ were considered statistically significant.

Results

Hep-2 cells infected with RSV

A single layer of adherent Hep-2 cells covered the bottom surface of the culture plates. The cells were arranged closely and regularly into the shape of polygons, like 'paving stones,' as observed under the light microscope. After the cells were infected with RSV A2 strain, typical fusion lesions (syncytia formations) could be viewed under the microscope. It was observed that the boundary of cells was indistinct, and cells with lesions fused into a 'multinucleated giant cell' syncytium (**Figure. 1**).

Inflammatory mediators in RSV-infected asthmatic mice

The total lung cells, as shown **Figure. 2 B** using Wright-Giemsa staining, showed that the control group (the PBS challenged group) had few eosinophils. In other group, the eosinophils in the bronchoalveolar lavage fluid of the OVA group was significantly higher than that in the PBS challenged group. In the OVA + RSV group, the total number of lung cells was significantly higher than that in OVA challenged group. One of the important features of the allergic asthma model is the production of ovalbumin-specific IgE upon induction. So, levels of IgE were measured in serum from ovalbumin challenged mice, and in the control and OVA + RSV groups. IgE levels in serum of mice from ovalbumin challenged mice were significantly higher than in control mice (PBS), and OVA + RSV groups mice had significantly higher IgE levels than the OVA challenged group (**Figure. 2 C**). To define the inflammatory changes in the established RSV-infected asthma model, pathological manifestation of the lung was evaluated by H&E staining. Compared with the control group mice, an obvious presence of inflammatory cells around the airways and vessels was observed in the OVA challenge group. The number of inflammatory cells present around the airways of asthmatic mice infected with RSV dramatically increased compared with the others group (**Figure. 2 D**).

Aggravation of AHR in RSV-infected asthmatic mice

RSV provoked aggravation effect on AHR in OVA-induced asthma model was evaluated. Our studies found that mild changes in airway resistance (RL) and lung dynamic compliance (Cdyn) were observed in control group mice. However, there was a significant enhancement of airway responsiveness in OVA-exposed and OVA + RSV group mice, with an obvious increase in RL and decrease in Cdyn compared with the control mice (*P< 0.05, **P<0.01). OVA + RSV group exhibited significantly aggravated airway responsiveness provoked by methacholine and decreased airway compliance compared with the OVA and the control group (*P< 0.05, **P< 0.01) (Figure. 3).

Histological changes in lungs of RSV-infected asthmatic mice

Our study showed that the OVA group developed inflammatory cell changes in peribronchial and perivascular infiltrates, such as eosinophils, neutrophils, and lymphocytes compared with the control group. The OVA + RSV group developed more pronounced inflammatory changes than the OVA group (Figure. 2 D). Goblet cell hyperplasia and mucus hyperproduction was evaluated by PAS staining (Fig. 4 A). The ovalbumin-challenged mice exhibited significantly increased hyperplasia and mucus production in comparison to the control group. RSV-infected asthmatic mice developed significantly aggravated goblet cell hyperplasia and mucus hyperproduction. Evaluation of lung peribronchial collagen deposition using VG staining (Figure. 4 B) on lungs from ovalbumin-challenged mice showed distinct collagen deposition. RSV-infected asthmatic mice had significantly increased peribronchial collagen deposition than the other groups.

Changes in interleukin cytokines in RSV-infected asthmatic mice

RSV-infection during asthma can induce the imbalance of interleukin cytokines, such as IL-5, IL-13, IL-25, and IL-33. The measurement of serum levels of IL-5, IL-13, IL-25, and IL-33 in the mice was carried out using ELISA. OVA-mediated asthma and RSV infection could give lead to an abnormal production of cytokines. As shown in Figure. 5, the serum levels of interleukins were higher in the OVA group and highest in the OVA + RSV group, compared with the CON group ($P < 0.05$ and $P < 0.01$, respectively).

The composition of the gut microbiome is altered after RSV-infection in asthmatic mice

The feces of mice were analyzed to investigate whether RSV-infection has an effect on the gut microbiota of asthmatic mice. The gut microbiota was visualized using a flower plot and community bar plot created using the sequencing data. The flower plot suggested that asthma and RSV infected asthma significantly altered the number of OTUs. There were 157 core OTUs in the three groups, and the number of OTUs in the OVA + RSV group was significantly reduced. (**Figure. 6 A**). From the community bar plot, it is possible to observe that there are differences among the three groups at the levels of phylum (**Figure. 6 B**), family (**Figure. 6 C**), and genus (**Figure. 6 D**).

Compared with the CON and OVA groups, the abundance of*Bacteroidetes* and *Firmicutes* was higher and lower, respectively, in OVA + RSV group. In this result, the eight DNA samples extracted (CON groups) did not have good quality; thus, only 7 samples were analyzed. From the OVA + RSV groups 1-4, the DNA extracted samples did not have good quality, so we could only analyze 5-8 samples after eliminating 1-4 data sets. In order to verify the quality of the reserved samples, we have verified it twice. Compared with the CON group, the abundance of both *Bacteroidetes* and *Firmicutes*was lower in OVA group, which may be due to the lower abundance of*Bacteroidales* _S24_7_group, *Bacteroidaceae* ,*Clostridiales* _vadinBB60_group, and *Lachnospiraceae* . Significant differences in abundance were observed for*Prevotellaceae* _UCG_001 and *Helicobacter* . Compared with the control group, the abundance of both *Bacteroidetes* and*Firmicutes* was higher in the RSV group, which may due to the growth of *Prevotellaceae* , *Porphyromonadaceae* ,*Bacteroidaceae,* and *Lachnospiraceae* . The significant abundance differences were verified for*Lachnospiraceae* _NK4A136_group, *Prevotellaceae* _UCG_001,*Alloprevotella* , *Desulfovibrio* , *Mucispirillum,* and*Alistipes* . Compared with the OVA group, the abundance of both*Bacteroidetes* and *Firmicute* s was higher in the OVA + RSV group, which may be due to the growth of*Bacteroidales* _S24_7_group, *Prevotellaceae* , and*Lachnospiraceae* . Significant differences were verified for*Prevotellaceae* _UCG_001, *Lachnospiraceae* _NK4A136_group,*Alloprevotella* , *Desulfovibrio* , *Mucispirillum* , and*Alistipes* .

The alpha exponential rarefaction curve of Chao1 index (**Figure. 7 A**) and Shannon index (**Figure. 7 B**) showed clear asymptotes, which indicates a near-complete sampling of the community. The boxplots of Chao1 index (**Figure. 7 C**) and Shannon index (**Figure. 7 D**) showed significant differences among the three groups. Beta diversity statistics using the Principal Coordinate Analysis (PCoA) revealed significant differences in the cluster patterns of gut microbial communities (**Figure. 8 A, B**).

Changes in the gut microbiota in RSV infected asthmatic mice

Multivariate statistical analysis (ANOVA) screened the top 10 genera with significant differences and high relative abundance, which are*Bryobacter, Gemmatimonas, Helicobacter, Lactobacillus, Massilia, Nocardioides, Prevoteliaceae* _UCG_001*, Sphingomonas* , and two uncultured bacteria (**Figure. 9**).

To identify key biomarkers that are differentially displayed between the three groups, we performed a statistical analysis using linear discriminant analysis effect size (LEfSe) analysis with linear discriminant analysis (LDA) to characterize different species between the groups.

From the **Figure. 10 A** , we found that the taxonomic levels from kingdom to genus correspond to the circles radiating from the inside out. In the cladogram, the red, green, and blue nodes represent the microbial taxa that play an important role in CON, OVA, and OVA + RSV groups, respectively.

In the LDA scores histogram, biomarkers with significant differences between groups are revealed, and the score values represent the influence degree of the corresponding taxa. As shown in **Figure. 10 B-D** , there

were 9, 9, and 8 differential bacterial taxa in CON, OVA, and OVA + RSV group, respectively, and 13 microbial taxa, namely*Prevotellaceae_UCG_001, Prevotellaceae, Alphaproteobacteria, Campylobacterales, Helicobacter, Helicobacteraceae, Epsilonproteobacteria, Bacteroidales_S24_7_group, Bacteroidetes, Bacteroidia, Actinbacteria, Proteobacteria,* and*Uncultured_Bacteroidales_bacterium. Prevotellaceae_UCG_001, Helicobacter,* and *Bacteroidales_S24_7_group* could serve as potential diagnosis and treatment biomarkers among the groups.

Alteration of gut microbiota associated with the levels of IgE and interleukins in RSV-infected asthmatic mice

To further verify the potential function of these core OTUs, we examined the reliability relationship between the core OTUs and IgE, cytokines including IL-5, IL-13, IL-25, IL-33, and found that 15 microbial OTUs were significantly associated with the IgE and inflammatory cytokines.*Prevotellaceae* _UCG_001, which is positive, was the most significantly associated with IgE, IL-13, and IL-33 ($P < 0.001$) and even more significantly associated with IL-5 ($P < 0.01$), IL-25 ($P < 0.05$).*Lachnospiraceae* _NK4A136_group was also positive, significantly associated with IgE ($P < 0.05$) and IL-33 ($P < 0.01$).*Helicobacter* and *Uncultured_Bacteroidales_bacterium,*which are negative, have a relevance and consistency with IL-25 ($P < 0.05$) (**Figure. 11**).

DISCUSSION

Globally, asthma currently affects the health of more and more people and this number is expected to increase to 400 million by 2025. Approximately 250,000 asthma-related deaths are reported yearly[26]. RSV related asthma is associated with worse severity, higher risk, intensive care, and mortality in some cases[27]. Some studies have shown that RSV[28], significantly altered gut microbiota diversity, with an increase in *Bacteroidetes* and a decrease in*Firmicutes* phyla abundance has been observed in RSV infected mice.

Gut microbiota play an important role in nutrient metabolism, immunomodulation, drug metabolism and xenobiotic/antimicrobial protection [11]. *Bacteroidetes* and*Firmicutes* comprise two major phyla of the normal human gut microbiota, and recent research suggests that the imbalance of the abundance and diversity in gut microbiota has a compact connection with alterations of airway microbiota and asthma, especially in children[29-30]. It is believed that the gastrointestinal tract (GIT) and respiratory tract share the same mucosal immune system, which is the one of the mechanisms of the gut-lung axis [31]. In this study, we focused on the changes of gut microbiota in RSV-infected asthma and characterized the abundance and diversity changes in the gut microbiota following RSV infection.

We discovered that OVA-challenged asthma led to a decrease in both the phylum of *Bacteroidetes* and *Firmicutes* . The two phyla exhibited an intense decrease after RSV infection, which even exceeded the normal group. According to the family and OTU levels,*Prevotellaceae* _UCG_001, *Lachnospiraceae* _NK4A136_group,*Alloprevotella* , *Desulfovibrio* , *Mucispirillum* , and*Alistipes* brought out the growth of*Bacteroidales* _S24_7_group, *Prevotellaceae* ,*Lachnospiraceae* , which supported a *Bacteroidetes* and*Firmicutes* blast. The unknown regulation of RSV resulting in*Bacteroidetes* and *Firmicutes* propagation is noteworthy and constitutes a part of our next study.

RSV is commonly responsible for acute respiratory disease in children and adults, and RSV infected asthmatic mice show enhanced the level of IgE in the serum [32-33]. Th2 cytokines, such as IL-5 and IL-13, play an important role in RSV-aggravated asthma[34-36]. The high level of IL-5 recruits and activates eosinophil proliferation. Increase in IL-13 levels induce AHR. RSV infected asthma can also provokes epithelium-derived cytokines, such as IL-25, IL-33, lead to inflammation, facilitate the development of asthma[37]. IL-33 enhances AHR and airway inflammation by suppressing antiviral responses [38]. Previous research suggested that virus infection induced airway hyper-reactivity through the IL-13-IL-33 axis pathway [39].

Gut microbiota has an impact on cytokines, and fecal microbiota transplantation in gut microbiota-depleted model mice led to a normalization of pulmonary bacterial counts [40]. In this study, we made a correlation analysis which showed that interleukins have a positive correlation with RSV infection with major different genus. Results showed that Prevotellaceae_UCG_001, which is positive, was the most significantly associa-

ted with IgE, IL-13, and IL-33 ($P < 0.001$) and even more significantly associated with IL-5 and IL-25. Lachnospiraceae_NK4A136_group was also positive, significantly associated with IgE and IL-33 ($P < 0.01$). Helicobacter and Uncultured_Bacteroidales_bacterium, which are negative, have a relevance and consistency with IL-25 ($P<0.05$). Prevotellaceae_UCG_001 and Lachnospiraceae_NK4A136_group especially expressed a significant correlation with interleukins, which suggested potential therapeutic targets on RSV-infected asthmatic following alteration of gut microbiota. Meanwhile, *Prevotellaceae* _UCG_001 and*Lachnospiraceae* _NK4A136_group were selected for potential therapeutic targets, having presented significant differences following RSV infection.

In summary, differences in the gut microbiota between healthy children and children with pediatric chronic respiratory diseases, including respiratory infection, asthma, and chronic pulmonary disease, suggest that the gut microbiota may play a crucial role in the development of these diseases. RSV infection Asthma of children is associated with a dysbiosis of the gut microbiota, which is marked by a general decline in beneficial potential microbiota, but can lead to an enrichment of potentially pathogenic taxa. These changes in the gut microbiota might disrupt the gut barrier integrity and enhance gut-lung inflammation.

Ethics statement

All animal protocols used in this study were approved by the Institutional Animal Care and Use Committee of Shanghai Jiao Tong University (approval No. 2016001).

ConFLict of interest

The authors declare no conflicts of interest regarding the study or the preparation of the manuscript.

Acknowledgements

This work was supported by the National Natural Science Foundation of China (Grant No. 81674020 to P J). The funders had no role in the study design, data collection and analysis, decision to publish, or preparation of the manuscript.

References

1. Global Initiative for Asthma. Global Strategy for Asthma Management and Prevention, 2020. Available from: www.ginasthma.org

2. Lai CK, Beasley R, Crane J, Foliaki S, Shah J, Weiland S. Global variation in the prevalence and severity of asthma symptoms: phase three of the International Study of Asthma and Allergies in Childhood (ISAAC). Thorax. 2009; 64(6):476-83.

3. Mattiuzzi C, Lippi G. Worldwide asthma epidemiology: insights from the Global Health Data Exchange database. Int Forum Allergy Rhinol. 2020; 10(1):75-80.

4. The editorial board of Chinese Journal of Pediatrics respiratory group. Pediatric Society of Chinese medicine, children's asthma Guidelines for diagnosis and treatment (2016 Edition). Chinese J Pediatr. 2016; 54(3):167-81. (Chinese)

5. Nyiro JU, Munywoki P, Kamau E, et al. Surveillance of respiratory viruses in the outpatient setting in rural coastal Kenya: baseline epidemiological observations. Wellcome Open Res. 2018 3:89.

6. Rezaee F, Linfield DT, Harford TJ, et al. Ongoing developments in RSV prophylaxis: a clinician's analysis. Curr Opin Virol. 2017; 24:70-8.

7. Jartti T, Gern JE. Role of viral infections in the development and exacerbation of asthma in children. J Allergy Clin Immunol. 2017; 140(4):895-906.

8. Piedimonte G. Contribution of neuroimmune mechanisms to airway inflammation and remodeling during and after respiratory syncytial virus infection. Pediatr Infect Dis J. 2003; 22(2 Suppl):S66-74; discussion S-5.

9. Tan YR, Yang T, Liu SP, et al. Pulmonary peptidergic innervation remodeling and development of airway hyperresponsiveness induced by RSV persistent infection. Peptides. 2008; 29(1):47-56.

10. Eckburg PB, Bik EM, Bernstein CN, et al. Diversity of the human intestinal microbial flora. Science (New York, NY). 2005; 308(5728):1635-8.

11. Jandhyala SM, Talukdar R, Subramanyam C, et al. Role of the normal gut microbiota. World journal of gastroenterology. 2015; 21(29):8787-803.

12. Arrieta MC, Stiemsma LT, Dimitriu PA, et al. Early infancy microbial and metabolic alterations affect risk of childhood asthma. Science translational medicine. 2015; 7(307):307ra152.

13. Stokholm J, Blaser MJ, Thorsen J, et al. Maturation of the gut microbiome and risk of asthma in childhood. Nature communications. 2018; 9(1):141.

14. Guan WJ, Ni ZY, Hu Y, et al. Clinical Characteristics of Coronavirus Disease 2019 in China. N Engl J Med. 2020; 382(18):1708-20.

15. Sze MA, Tsuruta M, Yang SW, et al. Changes in the bacterial microbiota in gut, blood, and lungs following acute LPS instillation into mice lungs. PLoS One. 2014; 9(10):e111228.

16. Sun Y, Lopez CB. Preparation of Respiratory Syncytial Virus with High or Low Content of Defective Viral Particles and Their Purification from Viral Stocks. Bio Protoc. 2016; 6(10). Epub 2016/05/20.

17. Xiaoping Jing, Wuning Yan, Hairong Zeng, et al. Qingfei oral liquid alleviates airway hyperresponsiveness and mucus hypersecretion via TRPV1 signaling in RSV-infected asthmatic mice. Biomedicine & Pharmacotherapy. 2020; 128:110340.

18. Reyon D, Tsai SQ, Khayter C, et al. FLASH assembly of TALENs for high-throughput genome editing. Nature biotechnology. 2012; 30(5):460-465.

19. Bolger AM, Lohse M, Usadel B. Trimmomatic: a flexible trimmer for Illumina sequence data. Bioinformatics (Oxford, England). 2014; 30(15):2114-20.

20. Caporaso JG, Kuczynski J, Stombaugh J, et al. QIIME allows analysis of high-throughput community sequencing data. Nature methods. 2010; 7(5):335-6.

21. Edgar RC, Haas BJ, Clemente JC, et al. UCHIME improves sensitivity and speed of chimera detection. Bioinformatics (Oxford, England). 2011; 27(16):2194-200.

22. Rognes T, Flouri T, Nichols B, et al. VSEARCH: a versatile open source tool for metagenomics. Peer J. 2016; 4:e2584.

23. Wang Q, Garrity GM, Tiedje JM, et al. Naive Bayesian classifier for rapid assignment of rRNA sequences into the new bacterial taxonomy. Applied and environmental microbiology. 2007; 73(16):5261-7.

24. Chao A, Bunge J. Estimating the number of species in a stochastic abundance model. Biometrics. 2002 58(3):531-539.

25. Hill TC, Walsh KA, Harris JA, et al. Using ecological diversity measures with bacterial communities. FEMS microbiology ecology. 2003; 43(1):1-11.

26. Christiansen SC, Zuraw BL. Treatment of Hypertension in Patients with Asthma. N Engl J Med. 2019; 381(11):1046-57.

27. Ritchie AI, Farne HA, Singanayagam A, et al. Pathogenesis of Viral Infection in Exacerbations of Airway Disease. Annals of the American Thoracic Society. 2015; 12 Suppl 2:S115-32. Epub 2015/11/26.

28. Rangelova E, Wefer A, Persson S, et al. Surgery Improves Survival After Neoadjuvant Therapy for Borderline and Locally Advanced Pancreatic Cancer: A Single Institution Experience. Annals of surgery. 2019; Epub 2019/04/05.

29. Lee-Sarwar KA, Kelly RS, Lasky-Su J, et al. Integrative analysis of the intestinal metabolome of childhood asthma. J Allergy Clin Immunol. 2019; 144(2):442-54.

30. Sharma A, Laxman B, Naureckas ET, et al. Associations between fungal and bacterial microbiota of airways and asthma endotypes. J Allergy Clin Immunol. 2019; 144(5):1214-27.e7.

31. Budden KF, Gellatly SL, Wood DL, et al. Emerging pathogenic links between microbiota and the gut-lung axis. Nature reviews Microbiology. 2017; 15(1):55-63.

32. Jia Wang, Jinfeng Wu, Lingwen Kong, et al. BuShenYiQi Formula strengthens Th1 response and suppresses Th2-Th17 responses in RSV-induced asthma exacerbated mice. Journal of Ethnopharmacology. 2014; 154(1):131-47.

33. Qiong Qiong Xing, Li-Wei Liu, Xia Zhao, et al. Serum proteomics analysis based on label-free revealed the protective effect of Chinese herbal formula Gu-Ben-Fang-Xiao. Biomedicine & Pharmacotherapy. 2019; 119:109390.

34. Yoon H-K, Shim Y-S, Kim P-H, et al. The TLR7 agonist imiquimod selectively inhibits IL-4-induced IgE production by suppressing IgG1/IgE class switching and germline ε transcription through the induction of BCL6 expression in B cells. Cell Immunol. 2019; 338:1-8.

35. Ito R, Maruoka S, Soda K, et al. A humanized mouse model to study asthmatic airway inflammation via the human IL-33/IL-13 axis. JCI Insight. 2018; 3(21).

36. Ikutani M, Ogawa S, Yanagibashi T, et al. Elimination of eosinophils using anti-IL-5 receptor alpha antibodies effectively suppresses IL-33-mediated pulmonary arterial hypertrophy. Immunobiology. 2018; 223(6-7):486-92.

37. Gauvreau GM, O'Byrne PM, Boulet LP, et al. Effects of an anti-TSLP antibody on allergen-induced asthmatic responses. N Engl J Med. 2014; 370(22):2102-10.

38. Ravanetti L, Dijkhuis A, Dekker T, et al. IL-33 drives influenza-induced asthma exacerbations by halting innate and adaptive antiviral immunity. J Allergy Clin Immunol. 2019; 143(4):1355-70.e16.

39. Chang YJ, Kim HY, Albacker LA, et al. Innate lymphoid cells mediate influenza-induced airway hyper-reactivity independently of adaptive immunity. Nature immunology. 2011; 12(7):631-8.

40. Schuijt TJ, Lankelma JM, Scicluna BP, et al. The gut microbiota plays a protective role in the host defence against pneumococcal pneumonia. Gut. 2016; 65(4):575-583.

Figure Legends

Figure 1 Manifestation of Respiratory Syncytial Virus infected Hep-2(human laryngeal carcinoma) cells

Hep-2 cells formed 'paving stones' shapes, which adhered to the surface of culture plates. The cells formed a 'multinucleated giant cell' syncytium after the infection by the RSV A2 strain. CON, control; RSV, respiratory syncytial virus.

Figure 2 Inflammatory mediators in RSV-infected asthmatic mice

(a) Schematic of experiment for RSV-infected asthma model. (b) Eosinophils in the bronchoalveolar lavage fluid shown using Wright-Giemsa staining. (c) RSV-infected increase in IgE level in serum as determined by ELISA. (d) Inflammatory changes within lungs were measured by H&E staining (×200). Values are presented as mean ± SD (n=3). ***P<0.001 compared to the control group and ***P<0.001 compared with the control group.

Figure 3 Effect of RSV-infection on Airway resistance and compliance in asthmatic mice

RSV infections further aggravated AHR to methacholine in OVA-challenged mice. RSV-induced asthma could change AHR in asthma exacerbated mice. Airway responsiveness to methacholine (3.125, 6.25, 12.5 mg/mL) was evaluated by a Buxco's modular and invasive system. (A) Changes in RL. (B) Changes in Cdyn. The data are expressed as the mean ± S.E.M. *P<0.05, **P<0.01, versus the control group, (n=3).

Figure 4 Effect of RSV-infection on the histomorphology of lung tissues

As shown in HE sections of the lung tissue, typical interstitial pneumonia seriously narrowed the alveolus cavity, inflammatory infiltration, telangiectasia, and hyperemia in OVA + RSV group. PAS and VG staining revealed that the OVA + RSV group exhibited the highest level of airway mucus secretion. CON, control; OVA, ovalbumin; RSV, respiratory syncytial virus; HE, hematoxylin and eosin staining; PAS, periodic acid-Schiff staining; VG, Van Gieson staining.

Figure 5 The levels of inflammatory factors in RSV infected asthmatic mice

Inflammatory factor levels of mice serum were evaluated in the three groups using ELISA. Results are presented as mean ± SD values. Serum levels of inflammatory factors (IL-25 and IL-33) in OVA group were remarkably higher than the control group (*P < 0.05), while serum levels of inflammatory factors (IL-5, IL-13, IL-25, and IL-33) in the RSV+ OVA group were significantly higher than the OVA group (#P < 0.05) and the control group (**P < 0.01). SD, standard deviation; CON, control; OVA, ovalbumin; OVA + RSV, respiratory syncytial virus + ovalbumin.

Figure 6 Composition of the gut microbiota is altered in RSV infected asthmatic mice

Flower plot (**A**) shows the number of OTUs of each sample and the number of common and unique OTUs of different samples. There are 157 core OTUs of three groups. The number of OTUs of RSV + OVA group was significantly reduced. Based on the results of relative abundance of statistical analysis, the community plot reflects the community structure of different samples (groups) at the phylum (**B**), family (**C**), and genus (**D**) levels. CON, control; OVA + RSV, respiratory syncytial virus + ovalbumin.

Figure 7 Alpha rarefaction curve and Boxplot analysis

Alpha index rarefaction curve can show the difference of species abundance among samples and evaluate the rationality of sequencing quantity of samples. Boxplot analysis of alpha diversity using Kruskal Wallis test reflected the dispersion degree of samples in the group and the inter group index differences. Chao1 index (**A, C**) reflected richness and Shannon (**B, D**) index considered the diversity. CON, control; OVA, ovalbumin; OVA + RSV, respiratory syncytial virus + ovalbumin.

Figure 8 Beta diversity (PCoA) of the three groups

The similarity and difference of species composition among different individuals or groups using PCoA with Bray Curtis. Results display that there are differences in the composition of three groups. CON, control; OVA, ovalbumin; OVA + RSV, respiratory syncytial virus + ovalbumin. A: Unweighted pair-group method with arithmetic means (UPGMA) hierarchical clustering graph. B: Results display that there are differences in the composition of the three groups. CON, control; OVA, ovalbumin; OVA + RSV, respiratory syncytial virus + ovalbumin.

Figure 9 Tested significant different genera using multivariate statistical analysis (ANOVA)

The top 10 different genera were selected using multivariate statistical analysis (ANOVA) among the three groups. CON, control; OVA, ovalbumin; OVA + RSV respiratory syncytial virus + ovalbumin.

Figure 10 The comparison of inter-group variance at relative abundance level using LEfSe analysis.

(A) The taxonomic cladogram. The diameter of the circle represents the relative abundance in the cladogram. The species with no significant difference are uniformly colored in yellow, and the species with significant difference are colored using the biomarker of the following group. A significant value lower than 0.05 was

used as a threshold for the LEfSe. (B-D) The histogram of LDA scores; CON, control; OVA, ovalbumin; OVA + RSV (respiratory syncytial virus + ovalbumin).

Figure 11 Correlation analysis between interleukins and different genera

Correlation analysis between IgE, IL-5, IL-13, IL-25, and IL-33 and the major genera. The analysis was done using Spearman test and the maximum correlation coefficient was $R^2 = 0.8$. Red represents a positive correlation and blue a negative correlation; the deeper the color, the better the correlation.

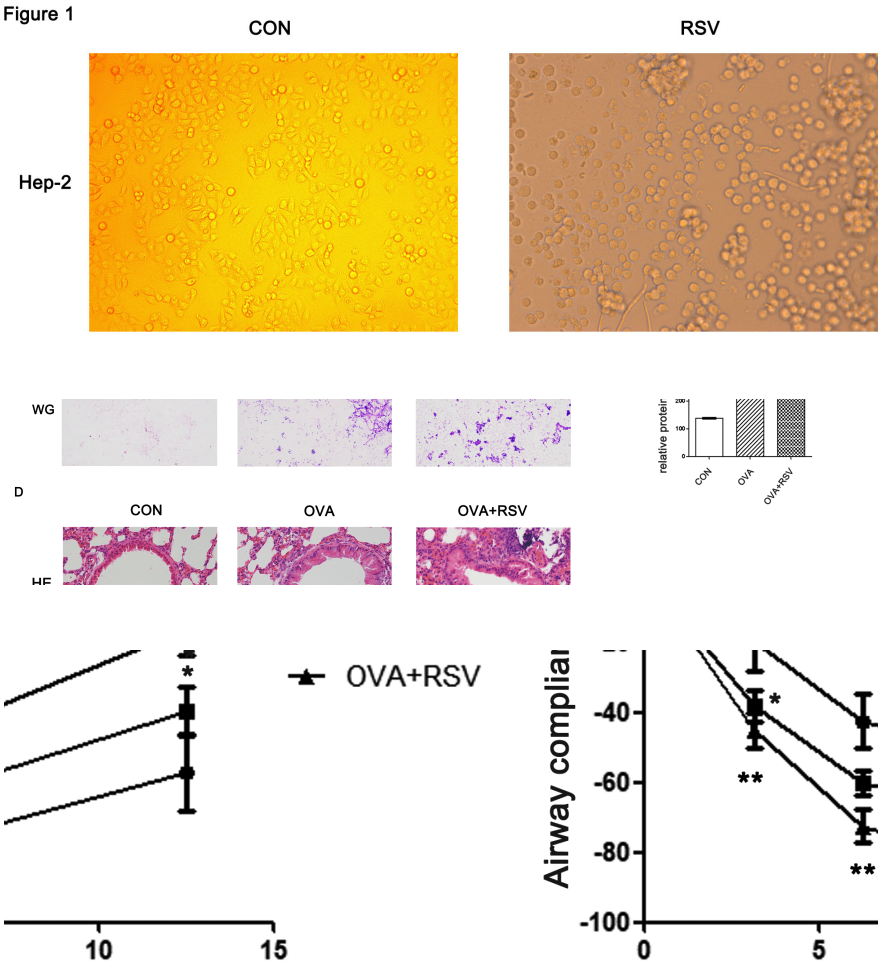

Figure 4

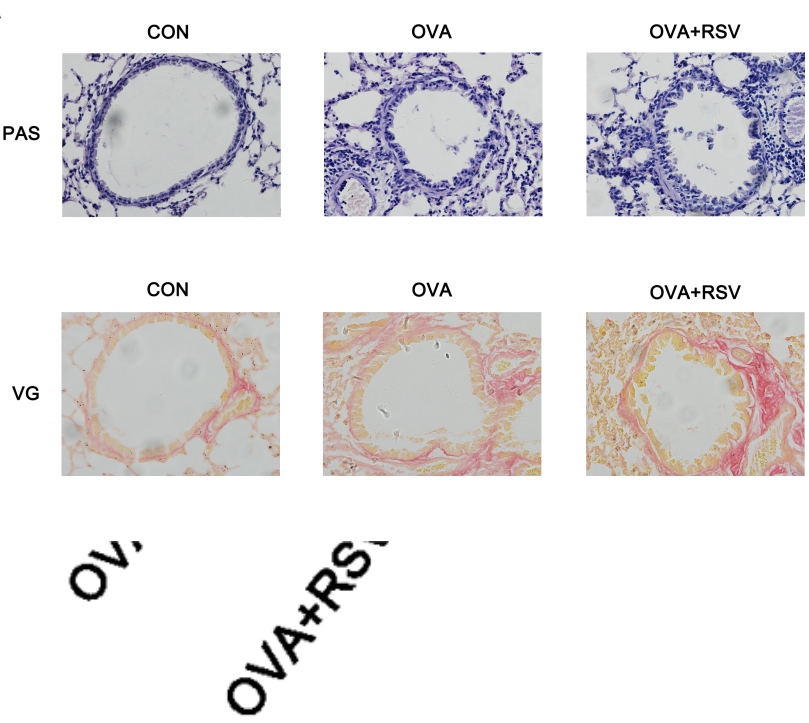

Figure 6

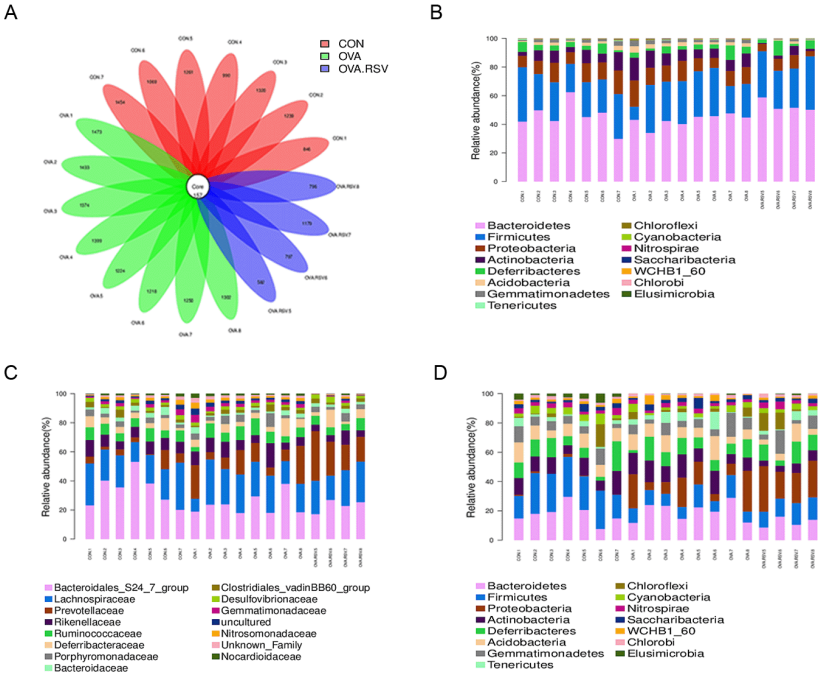

Figure 7

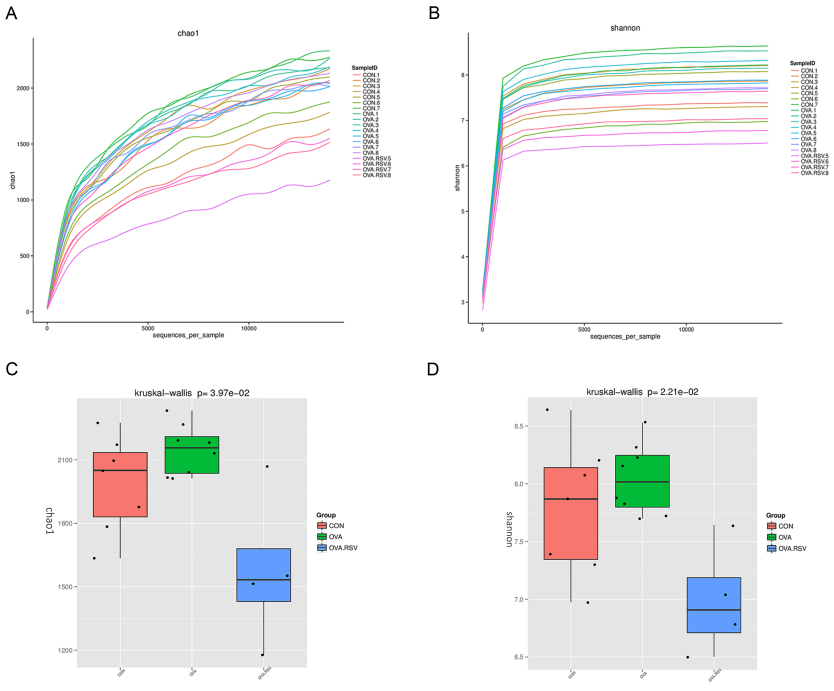

Figure 8

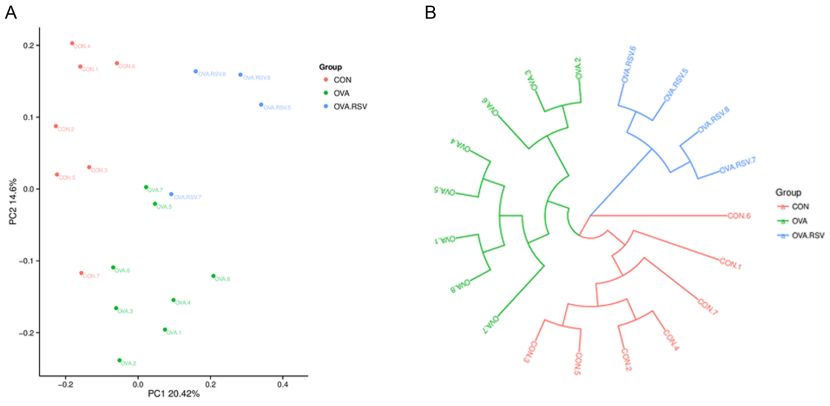

Figure 9

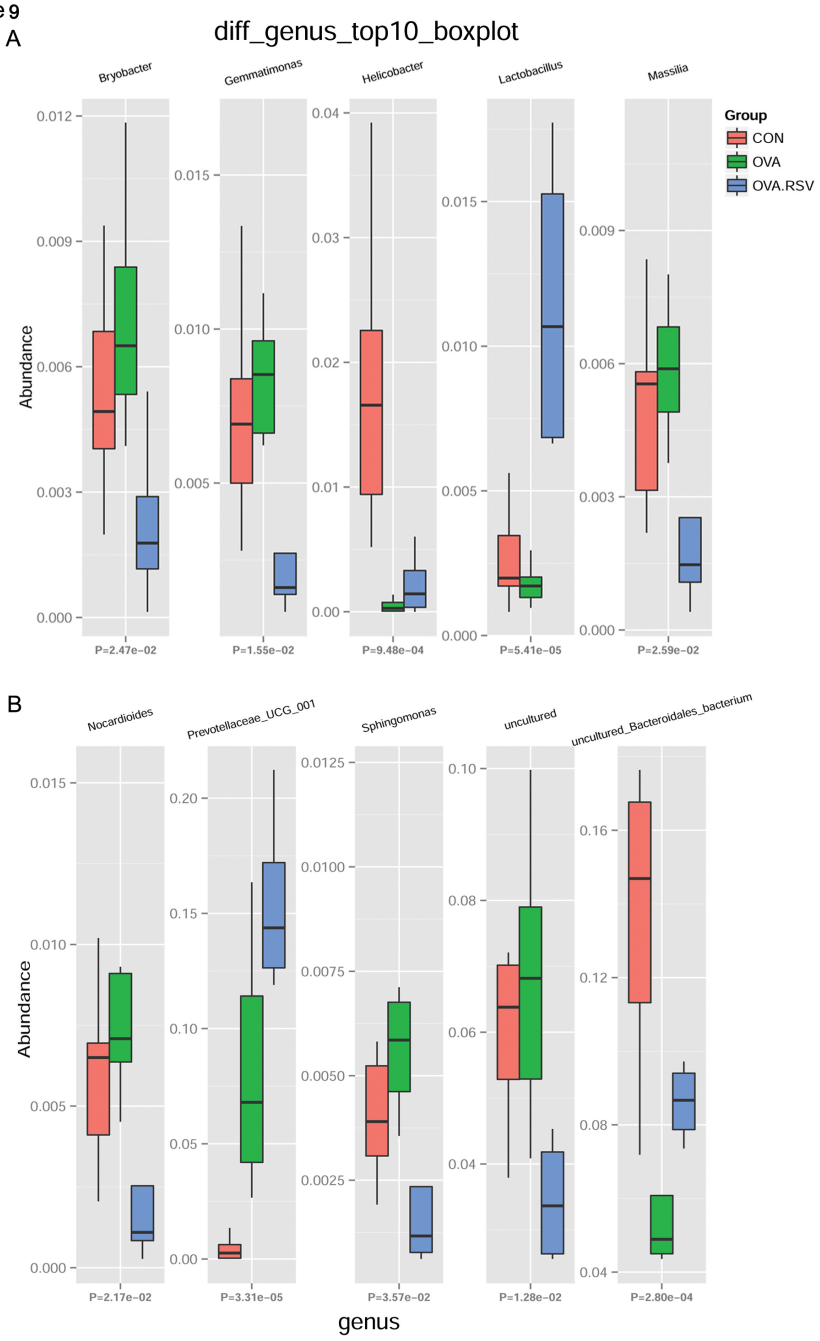

Figure10

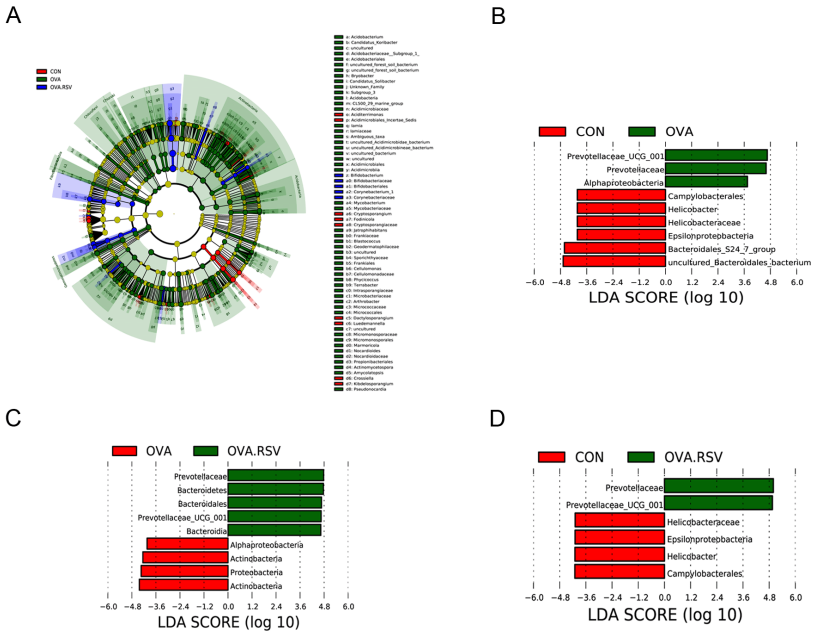

Figure 11